

THE UNUSUAL $\ddot{\Omega}$ OF THE MILLISECOND PULSAR 1620–26: THE CONSEQUENCE OF A GIANT GLITCH?

K. S., CHENG, N. CHONG, AND T. M. LEE

Department of Physics, University of Hong Kong, Pokfulam Road, Hong Kong

Received 1994 January 14; accepted 1994 April 27

ABSTRACT

We suggest that the unusually large second derivative of angular velocity of PSR 1620–26 may result from a recent giant glitch which occurred more than 30 yr ago, instead of being caused by a second companion orbiting around the binary system of the pulsar. Our model parameters predict that either the core magnetic field of this pulsar is much stronger than its surface magnetic field if the internal torque is produced by the core superfluid, or $\ddot{\Omega}$ is actually larger than the present upper limit by a factor of several if the internal torque is produced by the crustal superfluid. The former case will indicate that the internal magnetic fields of both the canonical pulsars and millisecond pulsars are the same. We further suggest that PSR 1620–26 should be a soft X-ray source with $L_x \sim 5 \times 10^{32}$ ergs $^{-1}$ and characteristic energy $E_\gamma \sim 200$ eV.

Subject headings: pulsars: individual (PSR 1620–26) — stars: magnetic fields

1. INTRODUCTION

The millisecond pulsar 1620–26 in the globular cluster M4 is in a binary system with a $0.3 M_\odot$ companion star. Subsequent measurements of this pulsar were analyzed (Lyne 1988; McKenna & Lyne 1988), and the data can be fitted by a polynomial function of time, with terms for spin frequency Ω and the spin-down rate $\dot{\Omega}$. The residuals of the data of this pulsar can be removed by a simultaneous fit for an unusually large $\ddot{\Omega} = 1.2 \times 10^{-22}$ s $^{-3}$, which is seven orders of magnitude larger than that predicted by pure dipole radiation, and the third derivative $\ddot{\Omega}$ of the spin rate (Backer, Foster, & Sallmen 1993, and references therein). Because the $\ddot{\Omega}$ term is strongly coupled with other spin parameters, Backer et al. (1993) used 3 times the fitted value, i.e., $\ddot{\Omega} = 1.3 \times 10^{-31}$ s $^{-4}$, as an upper limit. Soon they considered several possible explanations, both intrinsic and extrinsic, for the unusual second derivative $\ddot{\Omega}$ of the spin rate. They found that it could be well explained by the presence of a second weakly bound companion object moving in a wide orbit around the main binary system. This third object may have been captured into this binary system during a recent collision with another stellar system (Sigurdsson 1993). In their calculations, a set of circular orbits with inclination angle 45° is considered. The values of the first derivative can be suitably chosen to be consistent with the upper limit of $\ddot{\Omega}$. The ratio of the first and third derivatives of Ω would provide them with an exact value of the orbital period, and hence they could obtain the mass of the second companion star. Unfortunately, Backer et al. have only an *upper limit* of both quantities, which makes the corresponding mass of 2×10^{31} g and orbital period of 120 yr only estimates. By using the values obtained, the lower mass models which have been investigated in detail by Sigurdsson (1993) can provide favorable values of eccentricity and longitude of periastron necessary to keep the expected value of Ω below the limit Backer et al. set.

Their model has one great difficulty in the low binding energy of the second companion star in a wide orbit around the binary system. The pulsar's low-mass companion can be easily ejected from the system in an exchange encounter with other stars in the globular cluster. The collision time for the

disruption of this outer orbit, during which this pulsar system crosses the cluster hundreds of times, is of the order of 10^8 yr, which is also the lower limit to the age of the pulsar. It appears that such a scenario is acceptable, but certainly not the unique solution.

In this paper, we propose that such an unusually large $\ddot{\Omega}$ could be produced by the interaction between the solid part and the internal superfluid of the star if there is a glitch that occurred more than 30 yr ago. In § 2, we give a brief review of thermal vortex creep theory, which describes the interaction between the superfluid and the stellar crust. The temperature dependence of the relevant relaxation times are given. In § 3, we discuss how the energy released by a glitch can heat up the star. It turns out that the surface temperature is sensitive to the equations of state used. The observed values are compared with the model results, and the implications of model parameters will be discussed in § 4. Finally, a brief conclusion is drawn in § 5.

2. SUMMARY OF VORTEX CREEP MODELS

Although the details of neutron star structure sensitively depend on the neutron matter equation of state (EOS), the general structure of the star (Baym & Pethick 1979; Pines 1980) is adapted as follows: A solid outer crust of increasing mass density (7×10^6 g cm $^{-3} \lesssim \rho \lesssim 4 \times 10^{11}$ g cm $^{-3}$) contains a solid array of fully ionized nuclei and highly degenerate relativistic electron plasma (Ruderman 1969). An inner crust consists of a lattice of increasingly neutron-rich nuclei and relativistic electrons at density 4×10^{11} g cm $^{-3} \lesssim \rho \lesssim 2.4 \times 10^{14}$ g cm $^{-3}$, which coexist with a highly degenerate neutron superfluid liquid likely in an 1S_0 pairing state (Hoffberg et al. 1970; Yang & Clark 1971; Takatsuka 1972, 1984). In quantum liquid interior, the neutron-rich crustal nuclei have dissolved into free neutrons and protons which form a 3P_2 paired neutron superfluid and an 1S_0 paired superconducting fluid (Chao, Clark, & Yang 1972), respectively.

The rotating superfluid will form quantized vortex lines which are energetically favorable to pin to the nuclei of the crustal lattice. The pinning energy (E_p) is the gain in energy when a nucleon is inside the normal matter core of a vortex

line (Alpar 1977; Alpar, Cheng, & Pines 1989), which is given by

$$E_p = 0.87\gamma \Delta^2 k_F \text{ MeV}, \quad (1)$$

where γ is a dimensionless factor of order unity, Δ is the gap energy in units of MeV, and k_F is the Fermi wavenumber in units of fm^{-1} . Since the slow-down of the star due to magnetic dipole radiation sets up a differential rotation between the superfluid (with speed $v_s = r\Omega_s$) and the neutron vortices which are pinned to the crustal lattice and hence corotate with the star with speed $v_L = r\Omega$, this produces a Magnus force at the vortex line $f_M = \rho\kappa r(\Omega_s - \Omega)\hat{e}_r \equiv \rho\kappa r\omega\hat{e}_r$, where ω is the angular velocity lag between Ω_s and Ω . This force can reduce the pinning potential by $\Delta E = f_M b\xi$, where ξ is the coherent length of the superfluid and b is the distance between two pinning sites. The balance between the pinning force and the magnetic force defines the maximum (critical) lag between the angular velocities of the superfluid and of the crust given by

$$\omega_{\text{cr}} = 0.4\gamma \Delta r_6^{-1} k_F^{-1} b_Z^3 \text{ rad s}^{-1}, \quad (2)$$

where r_6 is in units of 10^6 cm and b_Z is the lattice spacing in units of 50 fm. For a system of superfluid vortices with azimuthal symmetry, the equation of motion of the superfluid angular velocity is given by

$$\dot{\Omega}_s = -\frac{\kappa n(r, t)v_r}{r} = -\frac{2\Omega_s v_r}{r}, \quad (3)$$

where $\kappa = h/m_n$ is the vorticity quantum, r is the distance from the rotation axis, n is the superfluid vortex density, and v_r is the radial velocity of the vortex line. In vortex creep models (Alpar et al. 1984a, b; Baym, Epstein, & Link 1992; Link, Epstein, & Baym 1993), the crust and the crustal neutron superfluid are assumed to be coupled primarily via the thermal creep of superfluid vortex lines; hence the thermal expectation value of the vortex velocity in the radial direction is simply given by

$$v_r = v_0 \{ \exp [-(E_p - \Delta E)/kT] - \exp [-(E_p + \Delta E)/kT] \}. \quad (4)$$

It has been argued by several authors (Sauls 1989; Srinivasan et al. 1990; Chau, Cheng, & Ding 1992) that, in the core, the magnetized vortex lines of the 3P_2 paired neutron superfluid are effectively pinned by the fluxoids of the 1S_0 paired proton superconducting fluid due to either the proton density perturbation in the center of a fluxoid ($E_p \sim 0.1\text{--}1$ MeV per connection) or the increase (or decrease) of magnetic energy in the interaction region ($E_p \sim 10$ MeV). Since the magnetic pinning energy is an order of magnitude larger than that of the proton density perturbation, we will only consider the former in the core superfluid. Chau et al. (1992) estimated that the pinning energy and the critical lag for the core superfluid were given by

$$E_p = 9.1 \times 10^7 \alpha \left(\frac{\delta m_p^*}{m_p} \right) (\chi_p \rho_{15})^{1/2} \ln \left(\frac{\Lambda}{\xi} \right) \cos \chi \text{ eV} \quad (5)$$

and

$$\omega_{\text{cr}} = 8.7 \times 10^{-2} \alpha r_6^{-1} \left(\frac{\delta m_p^*}{m_p} \right) \left(\frac{m_p^*}{m_p} \right)^{-1/2} \times \left(\frac{B_c}{10^{12} \text{ G}} \right)^{1/2} \ln \left(\frac{\Lambda}{\xi} \right) \chi_p \sin 2\chi \text{ rad s}^{-1}, \quad (6)$$

respectively. Here α is a geometrical factor of order unity, m_p^* ($=m_p - \delta m_p^*$) is the effective mass of a proton, B_c is the core magnetic field, χ_p is the proton concentration, ρ_{15} is the core density in units of $10^{15} \text{ g cm}^{-3}$, Λ is the penetration length, ξ is the coherent length of the proton superconducting fluid, and χ is the inclination angle.

The equation of motion for the crust is given by

$$I_{\text{ch}} \dot{\Omega} = N_{\text{ext}} + N_{\text{int}}, \quad (7)$$

where I_{ch} (the charged component) $\approx I_p$ is the moment of inertia of the crust (not including the crustal superfluid) plus that of the superconducting protons (I_p). N_{ext} is the external torque on the star, and

$$N_{\text{int}} = -\sum_{i=1}^2 I_{si} \dot{\Omega}_{si} \quad (8)$$

is the internal torque resulting from the crustal superfluid ($i=1$) and the core superfluid ($i=2$). In steady state, all the different components of the star should slow down at the same rate, namely, $\dot{\Omega} = \dot{\Omega}_{s1} = \dot{\Omega}_{s2} = \dot{\Omega}_\infty$, and $N_{\text{ext}} = I\dot{\Omega}_\infty$, where I is the total moment of inertia of the star. Combining equations (3), (4), (7), and (8) and ignoring the second term in equation (4), we obtain a differential equation for the lag (Alpar et al. 1989):

$$\dot{\omega} = |\dot{\Omega}_\infty| - \frac{1}{\eta} \exp \left(\frac{\omega}{\bar{\omega}} \right), \quad (9)$$

where $\eta = r|\dot{\Omega}_\infty| \exp(E_p/kT)/4\Omega_\infty v_0$ and $\bar{\omega} = \omega_{\text{cr}} kT/E_p$. The steady state lag is given by

$$\omega_\infty = \omega_{\text{cr}} \left[1 - \frac{kT}{E_p} \ln \left(\frac{4\Omega_\infty v_0}{r|\dot{\Omega}_\infty|} \right) \right] \simeq \omega_{\text{cr}}, \quad \text{for } \frac{kT}{E_p} \ll 1. \quad (10)$$

equation (10) indicates that the superfluid maintains a constant lag behind the charged component, but that they still couple together via thermal activation. Equation (9) can be solved easily (Alpar et al. 1989; Chau et al. 1992), and the observed behavior of the crust is given by

$$I_{\text{ch}} \dot{\Omega}(t) = I\dot{\Omega}_\infty - \sum_{i=1}^2 \frac{I_{si} \dot{\Omega}_\infty}{1 + [\exp(t_{oi}/\tau_i) - 1] \exp(-t/\tau_i)}, \quad (11)$$

where t_{oi} , the ‘‘dilation time’’ which characterizes the time when the superfluid and the crust star to couple, is given by

$$t_{oi} = \frac{I_{\text{ch}} \delta\omega_i(0)}{I |\dot{\Omega}_\infty|}, \quad (12)$$

$\delta\omega_i(0) = \omega_{i\infty} - \omega_i(0) \simeq \Delta\Omega$, and

$$\tau_i = \frac{kT}{E_{pi}} \frac{\omega_{\text{cri}}}{E_{pi} |\dot{\Omega}_\infty|}. \quad (13)$$

Here, we have assumed that the glitch occurs at $t=0$. We want to remark that the crustal superfluid ($i=1$) can actually have more than one relaxation time (Alpar et al. 1993).

3. INTERNAL HEATING BY A GLITCH

In this section, we discuss the thermal response of a pulsar to a glitch. The pioneer work on studying the thermal evolution following instantaneous heat release in a glitch has been done by Van Riper, Epstein, & Miller (1991).

It has been shown that a pulsar can achieve an isothermal core a few hundred to a thousand years after its formation

(Nomoto & Tsuruta 1981). Old pulsars like PSR 1620–26 should have an isothermal core if there has not been any sudden heating before. Energy liberated by glitches will disturb such isothermality. In this regard, cooling calculations have to take into account the spatial variations of temperature. An “exact” cooling model (Nomoto & Tsuruta 1987; Van Riper 1991) is then used. The methodological details of our cooling calculations are presented elsewhere (Chong & Cheng 1994).

The energy released by a glitch will modify the canonical cooling of a pulsar. Some rotating neutron stars have already been observed to undergo a sudden increase in their rate of rotation by about one part in 10^6 (the giant glitches), or by one part in 10^9 (the microglitches) (Manchester & Taylor 1977; Lyne & Graham-Smith 1989). The energy liberated in a giant glitch can be greater than $\sim 10^{43}$ ergs. This transient heating mechanism can occur anywhere inside the inner crust region by either sudden angular momentum transfer from the crustal superfluid to the solid part of the star (Pines & Alpar 1985) or sudden fracture of the crustal lattice due to gravitational stress (Baym & Pines 1971; Ruderman 1991a, b, c; Cheng et al. 1992; Chong & Cheng 1993a, b, 1994).

Glitches can be generated by the sudden transfer of angular momentum from the more rapidly rotating crustal superfluid to the solid crust region. Quantized vortex lines are believed to pin to the nuclei (Alpar et al. 1984a, b) and so cause a differential angular velocity and produce large strains in the crust. The energy dissipated from each glitch is $\Delta E \approx \Delta J \omega_{cr}$, where ΔJ is angular momentum transferred and ω_{cr} is the angular velocity lag between the crustal superfluid and the solid crust, which is proportional to the strength of pinning. At mass densities between 10^{13} and 2.4×10^{14} g cm $^{-3}$, the vortex lines strongly pin to nuclei, this region is called the nuclear pinning region (Alpar et al. 1984a, b). At lower densities between 10^{12} and 10^{13} g cm $^{-3}$, vortex lines repel nuclei and tend to pin to the lattice by threading a path between the nuclei; this region is called the interstitial pinning region (Epstein & Baym 1988). Van Riper et al. (1991) estimated that the ΔE from the nuclear pinning region is between 10^{41} and 10^{43} ergs and from the interstitial pinning region is $\sim 10^{40}$ ergs for canonical pulsars.

For crust cracking, the energy liberated can be approximated by $\Delta E = I\Omega^2(\Delta\Omega/\Omega)$, where I is the stellar moment of inertia, Ω is angular velocity, and $\Delta\Omega$ is the change in angular velocity due to the glitch. Therefore ΔE can be as large as 10^{45} ergs for millisecond pulsars, which have a canonical I of 10^{45} g cm 2 , $\Omega \sim 10^3$ rad s $^{-1}$, and $\Delta\Omega/\Omega \sim 10^{-6}$. The thermal response to $\Delta E = 10^{45}$ ergs is considered to be an extreme case of energy liberation which might happen if a millisecond pulsar has a Vela-like glitch.

We choose three EOSs to represent stellar models of varying “stiffness.” They are the EOS of Baym, Pethick, & Sutherland (1971; hereafter BPS), the EOS of Urbana VII plus the three-nucleon interaction model of Wiringa & Fiks (1988; hereafter UT), and the EOS of Panharipande, Pines, & Smith (1976; hereafter PPS). The stellar mass is chosen to be $1.4 M_{\odot}$.

Van Riper et al. (1991) have discussed soft X-ray pulses from neutron star after glitches. Our modeling runs for a UT star are comparable with their results, which were evaluated for $T_s \sim 10^{6.0}$ K. As we focus on the glitches to appear in the colder old pulsars, the core temperature is chosen to be 10^6 K (corresponding to $T_s \lesssim 10^5$ K) at which a much higher interior conductivity enables a fast thermal response to glitches—on a timescale of an hour, instead of days or months as for the hotter stars.

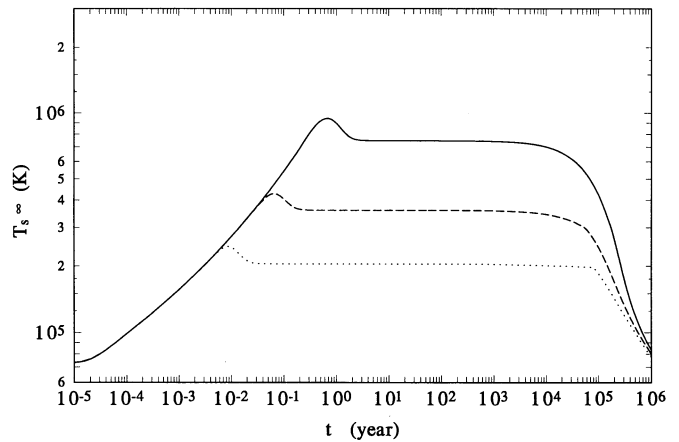


FIG. 1.—Evolution curves of surface temperature after a glitch. Solid line, dashed line, dotted line represent curves for $\Delta E = 10^{43}$, 10^{44} , and 10^{45} ergs, respectively. EOS is UT. The glitch occurs at $t = 0$.

Figure 1 shows the evolution curves of the surface temperature (T_s) for various glitch sizes. The initial core temperature is estimated to be $T_c \sim 10^6$ K by assuming that the core temperature is maintained by various internal heating mechanisms, i.e., vortex creeping (Alpar et al. 1984a, b; Shibasaki & Lamb 1989; Cheng et al. 1992) and/or continuous crust cracking (Chong & Cheng 1993a), which can maintain the core temperature around $[(1-3) \times 10^6$ K] for the parameters of PSR 1620–26. However, we want to remark that our results do not sensitively depend on the initial core temperature (cf. Fig. 4 of Chong & Cheng 1994).

The glitch is assumed to be activated at $\rho \sim 2 \times 10^{14}$ g cm $^{-3}$ when $t = 0$. We can see that the core temperature quickly rises to a maximum on a timescale of less than 1 yr and decreases relatively quickly over a timescale of ~ 1 yr. The high conductivity leads to the fast rising time, whereas neutrino emission activated by the sudden rise of temperature will eventually cool down the interior within a short period of time and also remove the nonisothermality inside the star. After that, the star resumes its isothermal core and radiates its heat content on a much longer timescale ($\gtrsim 10^4$ yr) by blackbody radiation. Figure 2 shows the evolution curves of the T_s -values for various

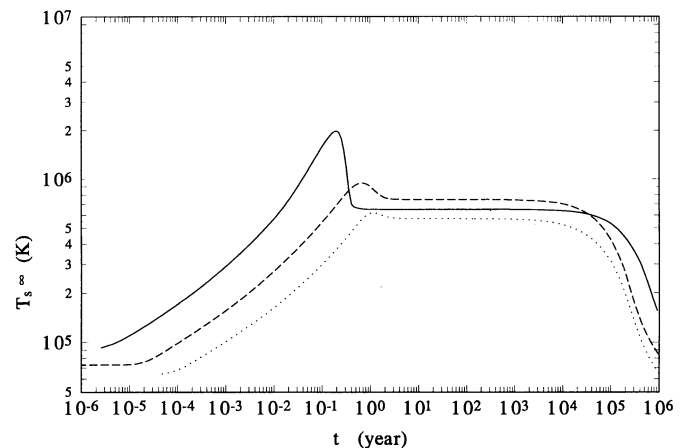


FIG. 2.—Evolution curves of surface temperature after a glitch, for $\Delta E = 10^{45}$ ergs. Solid line, dashed line, and dotted line represent curves for the EOSs BPS, UT, and PPS, respectively.

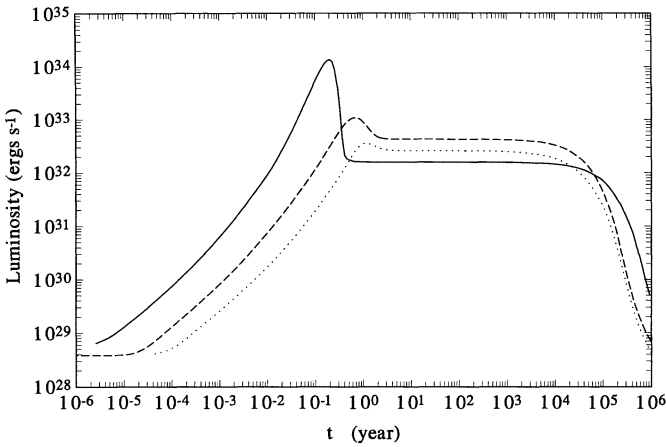


FIG. 3.—Evolution curves of the luminosity with respect to the cooling curves in Fig. 2.

EOSs. The behavior is similar to that in Figure 1. In Figure 3, we calculate the evolution curves of the luminosity of thermal X-rays with respect to the curves in Figure 2. Such thermal X-rays may be detectable by X-ray satellites.

4. EFFECT OF $\ddot{\Omega}$ AND $\dot{\Omega}$ ON MODEL PARAMETERS

There are a number of constraints on the timescales (t_{oi} and τ_i). Since the discovery of this pulsar, the timing data on Ω and $\dot{\Omega}$ do not show any peculiar behavior except an unusually large $\ddot{\Omega}$. This suggests that the glitch occurred before the discovery and the relaxation process has started but is not yet over, so

$$\tau_i \geq t \geq 6 \text{ yr} \geq t_{oi}, \quad (14)$$

where t is the time after the glitch. Although t could be larger than τ_i , in such a case the relaxation process should have been over before observation. Equations (12) and (14) imply the size of the glitch:

$$\frac{\Delta\Omega}{\Omega} \lesssim 8.2 \times 10^{-8} \left(\frac{I}{I_{\text{ch}}} \right). \quad (15)$$

Equation (11) can be approximated as

$$I_{\text{ch}} \dot{\Omega}(t) \simeq I \dot{\Omega}_{\infty} - \sum_{i=1}^2 I_{si} \dot{\Omega}_{\infty} \left(1 - \frac{t_{oi}}{\tau_i} e^{-t/\tau_i} \right). \quad (16)$$

The second and the third derivatives of Ω are given by

$$\ddot{\Omega} = \sum_{i=1}^2 \frac{I_{si}}{I_{\text{ch}}} |\dot{\Omega}_{\infty}| \frac{t_{oi}}{\tau_i^2} e^{-t/\tau_i} \quad (17)$$

and

$$\ddot{\Omega} = \sum_{i=1}^2 \frac{I_{si}}{I_{\text{ch}}} \dot{\Omega}_{\infty} \frac{t_{oi}}{\tau_i^3} e^{-t/\tau_i}, \quad (18)$$

respectively. The observed upper limit on $\ddot{\Omega}$ suggests that

$$\tau_i \approx \left| \frac{\ddot{\Omega}_{\text{obs}}}{\dot{\Omega}_{\text{obs}}} \right| \gtrsim 30 \text{ yr}. \quad (19)$$

(N.B. We want to point out that the observed data only give constraints on the absolute value of $\ddot{\Omega}$.) This puts a strong limit

on the relaxation time. We are going to consider the response from the crustal superfluid and the core superfluid separately.

4.1. Crustal Superfluid

The thermal relaxation time of the crustal superfluid is given by (Chau et al. 1992)

$$\tau_{\text{cr}} = 55 \text{ days } kT \text{ (keV)} / |\dot{\Omega}|_{-10} \Delta r_6 b_2^3 k_F^2, \quad (20)$$

where kT (keV) is the internal temperature in units of keV and $|\dot{\Omega}|_{-10}$ is the spin-down rate in units of 10^{-10} s^{-2} . From the cooling calculations (Figs. 1 and 2) 6 yr after the glitch with size $\Delta\Omega/\Omega \sim 10^{-6}$, the corresponding internal temperature, which is related to the surface temperature (Gudmundsson, Pethick, & Epstein, 1982) and to the redshift parameters (given for various EOSs in Chong & Cheng 1993a), is expected to be

$$kT \sim (4-7) \text{ keV}. \quad (21)$$

For PSR 1620-26, taking $|\dot{\Omega}|_{-10} = 5 \times 10^{-4}$ together with equation (21), we expect the relaxation to be

$$\tau_{\text{s,cr}} \sim (1-2) \times 10^3 \text{ yr}, \quad (22)$$

which is consistent with equations (14) and (19). However, equations (14) and (17) imply

$$\tau_{\text{s,cr}} \lesssim \frac{I_{\text{s,cr}} |\dot{\Omega}_{\infty}|}{I_{\text{ch}} |\ddot{\Omega}|} = 13.4 \frac{I_{\text{s,cr}}}{I_{\text{ch}}} \text{ yr}. \quad (23)$$

If the core superfluid has already coupled to the charged component, then $I_{\text{s,cr}}/I_{\text{ch}} \sim 1\%-40\%$ (Ditta & Alpar 1993). This violates the constraint of equation (19). The observed constraint on $\ddot{\Omega}$ suggests that the response may not come from the crustal superfluid. We want to point out that if further observation yields a $\ddot{\Omega}$ larger than the present value by a factor of several, then some very stiff EOSs would allow the response to come from the crustal superfluid.

4.2. Core Superfluid

The thermal relaxation for the core superfluid is given by (Chau et al. 1992)

$$\tau_c = 1 \text{ day } kT \text{ (keV)} |\dot{\Omega}|_{-10}^{-1} r_6^{-1} \left(\frac{\delta m_p^*}{m_p} \right)^{-1/2} \times \left(\frac{B_c}{10^{12} \text{ G}} \right)^{1/2} \left(\frac{\chi_p}{\rho_{15}} \right)^{1/2} \sin \frac{2\chi}{\cos \chi}. \quad (24)$$

Taking typical values of the parameters, $m_p^*/m_p \sim 0.5$, $r_6 \sim 1$, $\chi_p \sim 0.03$, $\rho_{15} \sim 0.02$, and $\chi = 45^\circ$, and $|\dot{\Omega}|_{-10} = 5 \times 10^{-4}$ for PSR 1620-24, equation (24) becomes

$$\tau_c \simeq 4.3 \text{ yr } kT \text{ (keV)} (B_c/10^{12} \text{ G})^{1/2} \quad (25)$$

$$= (17.2-30.1) (B_c/10^{12} \text{ G})^{1/2} \text{ yr}. \quad (26)$$

Here we have used equation (21). Again, the observed value of $\ddot{\Omega}$ imposes a serious constraint on τ_c , namely,

$$\tau_c \lesssim \frac{I_{\text{s,c}} |\dot{\Omega}|}{I_{\text{ch}} |\ddot{\Omega}|} \approx \left(\frac{I_{\text{s,c}}}{I_{\text{ch}}} \right) 13.4 \text{ yr}, \quad (27)$$

where $I_{\text{ch}} (= I_p + I_{\text{s,cr}})$ depends on the crustal superfluid and the charged component of the star. For various EOSs the

$I_{s,c}/I_{ch} \sim (2.5-10^2)$ satisfy the observed constraint of equation (19). However, this suggests that the core magnetic field is larger than the surface magnetic field by a factor of 300!

According to the recycled pulsar scenario (Alpar et al. 1982; Backus, Taylor, & Damaskheh 1982), PSR 1620–26 would accrete $0.02 M_{\odot}$ over a timescale of 10^7 yr for a moderately stiff EOS star. This amount of material may cover most of the stellar magnetic field. The means density of this accretion material layer is given by

$$\langle \rho \rangle \sim 3 \times 10^{13} R_6^{-2} \delta r_5 \delta M_* \text{ g cm}^{-3}, \quad (28)$$

where δr_5 is the thickness of the layer units of 10^5 cm and δM_* is the accretion mass in units of $0.02 M_{\odot}$. The corresponding conductivity for this layer (Flower & Itoh 1976, 1981) is approximately $\sigma \sim 10^{26} \text{ s}^{-1}$. The diffusion time for the magnetic field to pass through this layer is approximately

$$\tau_D \sim 4\pi(\delta r)^2 \sigma / c^2 \sim 3 \times 10^8 \text{ yr}, \quad (29)$$

which is longer than the spin-down age and the accretion time-scales. Another possible reason is the following: The surface magnetic field is actually 10^{12} G but confined in a much smaller region $\sim 10^6 (3 \times 10^9 / 10^{12})^{1/3}$ cm, or $\sim 10^5$ cm, because we can only infer the magnetic moment by the spin-down rate. According to the plate tectonic models (Ruderman 1991a, b, c), the magnetic moment of a pulsar will be diminished as a result of crustal plate motion. Both scenarios suggest that the core magnetic field can actually be higher than the deduced “surface” magnetic field.

5. DISCUSSION

We have shown that the unusually large $\dot{\Omega}$ of the millisecond pulsar 1620–26 may result from the internal torque produced by the interior superfluid as a result of a glitch. If the response to the glitch comes from the crustal superfluid, then $\dot{\Omega}$ must be larger than the present observed value, which needs to be confirmed by further observation. On the other hand, the $\dot{\Omega}$ of PSR 1620–26 may provide information about the core, especially, the strength of the core magnetic field and the internal temperature. Although the inferred core field is 300 times stronger than the surface magnetic field inferred by assuming the dipole moment occupies the whole star, there are at least two possible scenarios which can resolve the apparent discrepancy. This also provides a possible explanation for the two classes of magnetic field for the canonical pulsars and millisecond pulsars. If our model is correct, PSR 1620–26 would be a relatively strong soft X-ray emitter (Fig. 3). Such thermal X-rays may be detectable on Earth.

Finally, we want to point out that the exact value of $\dot{\Omega}$ is very uncertain because the residual of the timing data after fitting a polynomial up to the second derivative of Ω is too small. The reported best-fit value of $\dot{\Omega}$ can only be regarded as an estimated upper limit.

This work was partly supported by the UPGC grant of Hong Kong.

REFERENCES

- Alpar, M. A. 1977, Ph.D. thesis, Cambridge Univ.
 Alpar, M. A., Anderson, P. W., Pines, D., & Shaham, J. 1984a, *ApJ*, 276, 325
 ———. 1984b, *ApJ*, 278, 791
 Alpar, M. A., Chau, H. F., Cheng, K. S., & Pines, D. 1993, *ApJ*, 409, 345
 Alpar, M. A., Cheng, K. S., & Pines, D. 1989, *ApJ*, 346, 823
 Alpar, M. A., Cheng, A., Ruderman, M. A., & Shaham, J. 1982, *Nature*, 300, 728
 Backer, D. C., Foster, R. S., & Sallmen, S. 1993, *Nature*, 365, 817
 Baym, G., Epstein, R. I., & Link, B. 1992, *Physica B*, 178, 1
 Baym, G., & Pines, D. 1971, *Ann. Phys.*, 66, 816
 Baym, G., & Pethick, C. J. 1979, *ARA&A*, 17, 415
 Baym, G., Pethick, C. J., & Sutherland, P. G. 1971, *ApJ*, 170, 299
 Backus, P. R., Taylor, J. M., & Damaskheh, M. 1982, *ApJ*, 255, L63
 Chao, N. C., Clark, J. W., & Yang, C. H. 1972, *Nucl. Phys. A*, 179, 320
 Chau, H. F., Cheng, K. S., & Ding, K. Y. 1992, *ApJ*, 399, 213
 Cheng, K. S., Chau, W. Y., Zhang, L., & Chau, H. F. 1992, *ApJ*, 396, 135
 Chong, N., & Cheng, K. S. 1993a, *ApJ*, 417, 279
 ———. 1993b, 23d Internat. Cosmic Ray Conf. 1, 5
 ———. 1994, *ApJ*, in press
 Ditta, B., & Alpar, M. A. 1993, *A&A*, 275, 210
 Epstein, R. I., & Baym, G. 1988, *ApJ*, 328, 680
 Flower, E. G., & Itoh, N. 1976, *ApJ*, 206, 218
 ———. 1981, *ApJ*, 250, 750
 Gudmundsson, E. H., Pethick, C. J., & Epstein, R. J. 1982, *ApJ*, 272, 286
 Hoffberg, M., Glassgold, A. E., Richardson, R. W., & Ruderman, M. A. 1970, *Phys. Rev. Lett.*, 24, 775
 Link, B., Epstein, R. I., & Baym, G. 1993, *ApJ*, 403, 285
 Lyne, A. G. 1988, *Nature*, 332, 226
 Lyne, A. G., & Graham-Smith, F. 1989, *Pulsar Astronomy* (Cambridge: Cambridge Univ. Press)
 McKenna, J., & Lyne, A. G. 1988, *Nature*, 336, 226
 Manchester, R. N., & Taylor, J. H. 1977, *Pulsars* (San Francisco: Freeman)
 Nomoto, K., & Tsuruta, S. 1981, *ApJ*, 250, L19
 ———. 1987, *ApJ*, 312, 711
 Pandharipande, V. R., Pines, D., & Smith, R. A. 1976, *ApJ*, 208, 550
 Pines, D. 1980, *J. de Phys. Colloq.*, 41, C2/111
 Pines, D., & Alpar, M. A. 1985, *Nature*, 316, 27
 Ruderman, M. A. 1969, *Nature*, 223, 597
 ———. 1976, *ApJ*, 203, 213
 ———. 1991a, *ApJ*, 366, 261
 ———. 1991b, *ApJ*, 382, 576
 ———. 1991c, *ApJ*, 382, 587
 Sauls, J. A. 1989, in *Timing Neutron Stars*, ed. H. Ögelman, & E. P. G. Van der Heuvel (Dordrecht: Kluwer), 81
 Shibasaki, N., & Lamb, F. K. 1989, *ApJ*, 346, 808
 Sigurdsson, S. 1993, *ApJ*, in press
 Srinivasan, G., Bhattacharya, D., Muslimov, A. G., & Tsygan, A. I. 1990, *Current Sci.*, 59, 31
 Takatsuka, T. 1972, *Prog. Theor. Phys.*, 48, 1517
 ———. 1984, *Prog. Theor. Phys.*, 71, 1432
 Van Riper, K. A. 1991, *ApJ*, 75, 449
 Van Riper, K. A., Epstein, R. I., & Miller, G. S. 1991, *ApJ*, 381, L47
 Wiringa, R. B., & Fiks, V. 1988, *Phys. Rev. C*, 38, 1010
 Yang, C. H., & Clark, J. W. 1971, *Nucl. Phys. A*, 174, 49